16th World Conference on Earthquake Engineering, 16WCEE 2017

Santiago, Chile, January 9th to 13th 2017

Paper No. 2609

Registration Code: S-T1461961331

NUMERICAL ANALYSIS OF A STEEL CYLINDRICAL TANK WITH FIXED AND ISOLATED BASES TO STORE LIQUIDS

J. P. Cordone[(1)], J. L. Almazán[(2)], M. E. Tornello[(3)], A. E. Mirasso[(4)], G. Gioacchini[(5)], F. Calderón[(6)]

[(1)] *CeReDeTeC, Facultad Regional Mendoza, Universidad Tecnológica Nacional, Rodríguez 273, Mendoza, Argentina, juanpablo.cordone@frm.utn.edu.ar*
[(2)] *Department of Structural and Geotechnical Engineering, Engineering School, Pontificia Universidad Católica de Chile, Av. Vicuña Mackenna 4860, Santiago, Chile, jlalmaza@ing.puc.cl*
[(3)] *CeReDeTeC, Facultad Regional Mendoza, Universidad Tecnológica Nacional, Rodríguez 273, Mendoza, Argentina, mtornell@frm.utn.edu.ar*
[(4)] *IMERIS, Engineering School, Universidad Nacional de Cuyo, Centro Universitario Parque San Martín, Mendoza, Argentina, aemirasso@yahoo.com.ar*
[(5)] *CeReDeTeC, Facultad Regional Mendoza, Universidad Tecnológica Nacional, Rodríguez 273, Mendoza, Argentina, ggioacchini@frm.utn.edu.ar*
[(6)] *CeReDeTeC, Facultad Regional Mendoza, Universidad Tecnológica Nacional, Rodríguez 273, Mendoza, Argentina, panchocalderon1@hotmail.com*

Abstract

Tanks for hazardous liquid storage have proved to be vulnerable when destructive earthquakes appear. Their collapse leads to the spillage of the contained substances (flammable, explosive, toxic) negatively impacting in the surrounding environment and causing big economic losses for the region where they are located. This work`s goal is to determine the effectiveness of the systems of seismic isolation in supported cylindrical tanks, which store hazardous liquids, and to measure the incidence of certain parameters over the response. In order to achieve this, it is necessary to perform a parametric analysis of the response history, with multiple runs and with a high computational cost. Due to that, a simple and fast method, based on the resolution of the problem through an Euler-Lagrange Equation is proposed in this article. As isolation devices, friction isolators of single friction pendulum were used. As an input, earthquakes with both vibratory and impulsive seismic movement characteristics were used. Both a base fixed and a base isolated tank were modeled, and as study parameters, the slenderness ratio of the tank and the period and the friction coefficient of the seismic isolation system were modeled. The seismic responses in terms of displacements of the free surface of the contained liquid, displacements of the isolation system and the normalized base shear were determined. The results state that the isolation system reduces the maximum response in all cases, but it increases its effectiveness as the tank slenderness ratio increases. The slender tanks are shown to be very sensitive to the system isolation period, while the thick tanks are strongly conditioned in its response by the friction coefficient.

Keywords: seismic analysis, cylindrical tank, base isolation

1. Introduction

Tanks for hazardous liquid storage have proved to be vulnerable against destructive earthquakes, as the ones in Valdivia, Chile in 1960, Alaska, United States, in 1964, Northdrige, California, United States, in 1994, Kobe, Japan in 1995 and Kocaeli, Turkey in 1999, among others. Their collapse leads to the spillage of the contained substances, negatively impacting in the surrounding environment and causing big economic losses for the region where they are located. This motivates the seismic behavior study of the tanks, and the development of new techniques for their protection, such as the base seismic isolation.

The seismic behavior of tanks has been studied for several years by many authors. In 1933, Westergaard [1] determined the pressure distribution of an incomprehensible fluid over a rigid dam of vertical wall during an earthquake. Afterwards, in 1949 Jacobsen [2] he stated the potential speed of a tank with fluid inside and around it when an impulsive translational displacement is experienced in its base, depreciating the connective part of the acceleration. Years later, in 1957 and 1963, Housner [3, 4] performed an analysis of the hydrodynamic pressure, developed when a fluid in a rigid wall container is subject to horizontal accelerations, including impulsive and connective pressures, and showing simplified equations for containers of different shapes. In 1973, Veletsos [5] developed a simplified procedure so as to assess the dynamic forces induced by the lateral component of an earthquake, taking into account the tank flexibility effects, but considering the impulsive forces. Then, in 1981 and 1983, Haroun [6, 7] showed a method based in the mode overlapping of free lateral vibration so as to assess the flexibility influence of the wall in the tank seismic response.

The seismic isolation technique applied to tanks has also a background. In 1997, Malhotra [8] showed that the seismic response of isolated tanks is reduced considerably without a significant increase of the swell in a free surface. In 2001, Wang [9] performed tank numerical simulations with a friction pendulum system (FPS), verifying that its effectiveness increases the tank slenderness ratio. In 2002, Shrimali y Jangid [10] performed a parametric analysis both on a thick tank and on a slender tank, so as to measure the incidence of the isolation period, the damping and the fluency force of the isolation system over the peak response of the tank, under a bidirectional excitation, taking into consideration the interaction effects, which turned to be negligible. In 2008 and 2012, Panchal and Jangid [11, 12] studied the response in cases of near-failure earthquakes of isolated tanks, with two newly friction pendulum system (FPS) devices, one with a variable friction pendulum system (VFPS) and another one with a variable curvature friction pendulum system (VCFPS), showing a better behavior than the FPS with a friction coefficient and bending radius that are constant with the movement. In 2010, Abalı and Uçkan [13] performed a parametric analysis of tanks with FPS isolators, so as to measure the incidence of the isolation period, the tank aspect and the friction coefficient ratio, in the tank response, taking into account the variation of the axial loading over the isolation system, due to the overturning moment and the vertical acceleration, and finding that said variation must not be ignored, mainly in slender tanks subject to near-fault seisms. In 2014, Saha [14] performed a parametric analysis so as to assess the response of a thick tank and a slender tank, by using equal linear modeled isolators and in bilinear form, showing that the equal linear model overestimates the response of slender tanks.

The goal of this work is stating the effectiveness of the seismic isolating systems in tanks, and measuring the incidence of certain parameters (isolation period, friction coefficient and slenderness ratio) over the response. In order to achieve this, it is necessary to perform a parametric analysis of the response history, with multiple runs and with a high computational cost. Due to that, a simple and fast method, based on the resolution of the problem through an Euler-Lagrange Equation is proposed in this article.

2. Method

So as to achieve the goal that was set forth, the following steps are fulfilled: i) Choose a model representing the physical behavior of the system: Housner Model is used; ii) Find the differential equations governing the system: Euler-Lagrange Equation is set forth, which leads to two ordinary differential equations of second order; iii) Reduce the order of the differential equations: State Equation is used, which enables the change from two ordinary differential equations of second order to four ordinary differential equations of first order; iv) Integrate the differential equations: the Runge Kutta numerical integration method of order three at a constant pace is used.

2.1 Housner model

Housner model proposes that the hydrodynamic response of a tank-liquid system is characterized by the participation of two different contributions, called impulsive component and convective component. The impulsive component represents the part of the liquid that moves in unison with the tank walls. The convective component represents the liquid moving with a long period waving movement, in the upper part of the tank. These two components may be deemed as uncoupled, because there are significant differences in their natural periods.

In a tank supported on the floor, the waving amplitude is an indicator of the soil movement intensity. In the event a tank with its water-free surface is subject to a $\ddot{X}$(t) horizontal acceleration of the floor, the forces exerted over the tank by water are of two types. First, when the tank walls accelerate, they come and go, and one part of the water is forced to take part in this movement, which exerts a reactive force over the tank, which would exert a m_i mass rigidly connected to the tank at a h_i appropriate height. The m_i mass is fixed to h_i height so as that the horizontal force exerted by it is collinear with the resulting force exerted by the equivalent water. Second, the tank wall movement excites the water in oscillations, which subsequently exerts an oscillatory force over the tank. This oscillatory force is the same exerted by a m_c mass which may horizontally oscillate against a k_c restriction spring. The m_c mass corresponds to the main oscillation mode of water, which is the most important mode in most of the seismic problems. In the event the equivalent system is subject to $\ddot{X}$(t) floor seismic accelerations, the forces exerted over the tank by the m_i and m_c masses shall be the same that water would exert over the tank.

For a cylindrical tank of R radius, and H liquid height, the equations to obtain the model necessary parameters are:

$$m_i = M \, \frac{\tanh\left(\frac{1.732\, R}{H}\right)}{\left(\frac{1.732\, R}{H}\right)} \qquad (1) \qquad\qquad m_c = 0.835\, M \, \frac{\tanh\left(\frac{1.835\, H}{R}\right)}{\left(\frac{1.835\, H}{R}\right)} \qquad (2)$$

$$\omega_c{}^2 = 1.835\, \frac{g}{R} \tanh\left(\frac{1.835\, H}{R}\right) \qquad (3) \qquad\qquad k_c = \omega_c{}^2\, m_c = 4.032605\, \frac{m_c{}^2}{M}\, \frac{g\, H}{R^2} \qquad (4)$$

$$h_i = \frac{3}{8}\, H \qquad (5) \qquad\qquad h_c = H\left[1 - \left(\frac{R}{1.835\, H}\right) tanh\left(\frac{0.9175\, H}{R}\right)\right] \qquad (6)$$

Where: R = radius of the tank cylinder; H = liquid height; ρ = liquid density; m = ρ π R^2 H mass of the contained liquid; m_i = impulsive mass; m_c = convective mass; g = 9, 81 m/s^2 gravity acceleration; k_c = convective rigidity; h_i = impulsive height; h_c = convective height

2.2 Euler – Lagrange equation

The Euler - Lagrange equation is obtained by applying the Principle of the Virtual Works to the Second Newton Law. The Principle of Virtual Works (PTV) states that “In a mechanical system, it is a necessary and sufficient condition of equilibrium that the work of the group of forces applied over virtual movements compatible with the bond be null”. For a system of *M* material points, the total virtual work is:

$$\delta W = \sum_{i=1}^{M} \boldsymbol{F}_i \cdot \delta \boldsymbol{r}_i = 0 \qquad (7)$$

On the other hand, the second Newton law states that:

$$\boldsymbol{F}_i = \dot{\boldsymbol{p}}_i \qquad (8)$$

where $\boldsymbol{p}_i$ is the *linear momentum* of the *i*-th particle. From expression (8), the following can be written:

$$\boldsymbol{\varphi}_i = \boldsymbol{F}_i - \dot{\boldsymbol{p}}_i = 0 \qquad (9)$$

where $\boldsymbol{\varphi}_i$ may be interpreted as the net force to be applied over the particle to keep it in “equilibrium”. Then, as in every instant, the system stays in equilibrium under the action of $\boldsymbol{\varphi}_i$ the principle of virtual works is fulfilled:

$$\sum_{i=1}^{M}\boldsymbol{\varphi}_i\cdot\delta\boldsymbol{r}_i=\sum_{i=1}^{M}(\boldsymbol{F}_i-\dot{\boldsymbol{p}}_i)\cdot\delta\boldsymbol{r}_i=\sum_{i=1}^{M}\boldsymbol{F}_i\cdot\delta\boldsymbol{r}_i-\sum_{i=1}^{M}\dot{\boldsymbol{p}}_i\cdot\delta\boldsymbol{r}_i=0 \tag{10}$$

By developing the first term of (10), we obtain:

$$\sum_{i=1}^{M}\boldsymbol{F}_i\cdot\delta\boldsymbol{r}_i=\sum_{i=1}^{M}\boldsymbol{F}_i\cdot\left(\sum_{j=1}^{N}\frac{\partial\boldsymbol{r}_i}{\partial q_j}\partial q_j\right)=\sum_{j=1}^{N}\sum_{i=1}^{M}\left(\boldsymbol{F}_i\cdot\frac{\partial\boldsymbol{r}_i}{\partial q_j}\right)\partial q_j=\sum_{j=1}^{N}Q_j\,\partial q_j \tag{11}$$

where q [Nx1] is the vector of system degree of freedom (GDL), with N as the number of degrees of freedom; and $Q_j=\sum_{i=1}^{M}\left(\boldsymbol{F}_i.\frac{\partial \boldsymbol{r}_i}{\partial q_j}\right)$ are the components of the generalized forces.

Next, the second term of (10) is developed:

$$\sum_{i=1}^{M}\dot{\boldsymbol{p}}_i\cdot\delta\boldsymbol{r}_i=\sum_{i=1}^{M}m_i\ddot{\boldsymbol{r}}_i\sum_{j=1}^{N}\frac{\partial\boldsymbol{r}_i}{\partial q_j}\partial q_j=\sum_{j=1}^{N}\sum_{i=1}^{M}\left(m_i\ddot{\boldsymbol{r}}_i\cdot\frac{\partial\boldsymbol{r}_i}{\partial q_j}\right)\partial q_j \tag{12}$$

From the inner product derivation, we have:

$$\frac{d\boldsymbol{a}}{dt}\cdot\boldsymbol{b}=\frac{d}{dt}(\boldsymbol{a}\cdot\boldsymbol{b})-\boldsymbol{a}\cdot\frac{d\boldsymbol{b}}{dt} \tag{13}$$

By using $\boldsymbol{a}=m_i\dot{\boldsymbol{r}}_i$ and $\boldsymbol{b}=\frac{\partial \boldsymbol{r}_i}{\partial q_j}$ the following is obtained:

$$\sum_{j=1}^{N}\sum_{i=1}^{M}\left\{\frac{d}{dt}\left(m_i\dot{\boldsymbol{r}}_i\cdot\frac{\partial\boldsymbol{r}_i}{\partial q_j}\right)-m_i\dot{\boldsymbol{r}}_i\frac{d}{dt}\left(\frac{\partial\boldsymbol{r}_i}{\partial q_j}\right)\right\}\partial q_j \tag{14}$$

If we consider the following equalities:

$$\frac{d}{dt}\left(\frac{\partial\boldsymbol{r}_i}{\partial q_j}\right)=\frac{\partial\dot{\boldsymbol{r}}_i}{\partial q_j} \tag{15}$$

$$\frac{\partial\boldsymbol{r}_i}{\partial q_j}=\frac{\partial\dot{\boldsymbol{r}}_i}{\partial\dot{q}_j} \tag{16}$$

Then, by replacing (15) and (16) in (14):

$$\sum_{j=1}^{N}\sum_{i=1}^{M}\left\{\frac{d}{dt}\left(m_i\dot{\boldsymbol{r}}_i\cdot\frac{\partial\dot{\boldsymbol{r}}_i}{\partial\dot{q}_j}\right)-m_i\dot{\boldsymbol{r}}_i\left(\frac{\partial\dot{\boldsymbol{r}}_i}{\partial q_j}\right)\right\}\partial q_j \tag{17}$$

Besides:

$$m_i\dot{\boldsymbol{r}}_i\cdot\frac{\partial\dot{\boldsymbol{r}}_i}{\partial\dot{q}_j}=\frac{\partial}{\partial\dot{q}_j}\left(\frac{1}{2}m_i\dot{\boldsymbol{r}}_i\cdot\dot{\boldsymbol{r}}_i\right)=\frac{\partial}{\partial\dot{q}_j}\left(\frac{1}{2}m_iv_i^2\right)=\frac{\partial T_i}{\partial\dot{q}_j} \tag{18}$$

$$m_i\dot{\boldsymbol{r}}_i\cdot\frac{\partial\dot{\boldsymbol{r}}_i}{\partial q_j}=\frac{\partial}{\partial q_j}\left(\frac{1}{2}m_i\dot{\boldsymbol{r}}_i\cdot\dot{\boldsymbol{r}}_i\right)=\frac{\partial}{\partial q_j}\left(\frac{1}{2}m_iv_i^2\right)=\frac{\partial T_i}{\partial q_j} \tag{19}$$

Where $T_i=\frac{1}{2}m_iv_i^2$ is the kinetic energy of the *i*-th particle. Then, by replacing (18) and (19) in (17):

$$\sum_{j=1}^{N}\sum_{i=1}^{M}\left\{\frac{d}{dt}\left(\frac{\partial T_i}{\partial\dot{q}_j}\right)-\frac{\partial T_i}{\partial q_j}\right\}\partial q_j=\sum_{j=1}^{N}\left\{\frac{d}{dt}\left(\frac{\partial T}{\partial\dot{q}_j}\right)-\frac{\partial T}{\partial q_j}\right\}\partial q_j \tag{20}$$

By replacing (11) in the first term of (10), and (20) in the second term of (10), the following is obtained:

$$\sum_{j=1}^{N}Q_j\,\partial q_j-\sum_{j=1}^{N}\left\{\frac{d}{dt}\left(\frac{\partial T}{\partial\dot{q}_j}\right)-\frac{\partial T}{\partial q_j}\right\}\partial q_j=0 \tag{21}$$

$$\sum_{j=1}^{N}\left\{\frac{d}{dt}\left(\frac{\partial T}{\partial\dot{q}_j}\right)-\frac{\partial T}{\partial q_j}-Q_j\right\}\partial q_j=0 \tag{22}$$

In the equation (22) Q_j may be divided as the sum of the conservative forces (derived from a potential function) and the non-conservative forces:

$$Q_j = Q_j^C + Q_j^{NC} = -\frac{\partial V}{\partial q_j} + \sum_{i=1}^{M} \boldsymbol{F}_i^{NC} \cdot \frac{\partial \boldsymbol{r}_i}{\partial q_j} \tag{23}$$

By replacing (23) in (22):

$$\sum_{j=1}^{N} \left[\frac{d}{dt}\left(\frac{\partial T}{\partial \dot{q}_j}\right) - \frac{\partial T}{\partial q_j} + \frac{\partial V}{\partial q_j} - Q_j^{NC}\right] \delta q_j = 0 \tag{24}$$

As the virtual movements are arbitrary, for fulfilling the equation (24), each term must be null, that is:

$$\frac{d}{dt}\left(\frac{\partial T}{\partial \dot{q}_j}\right) - \frac{\partial T}{\partial q_j} + \frac{\partial V}{\partial q_j} - Q_j^{NC} = 0 \tag{25}$$

The previous equation represents the sum of forces in equilibrium. In order to apply it, the total energy (kinetic energy called T and potential energy called V) of the system (cascade) and it is derived regarding the q generalized coordinates (minimum number of independent coordinates, needed to describe the system = number of degrees of freedom), and the Q^{NC} non-conservative forces are also added, so as to obtain, in this way, the differential equations governed by the system.

The steps to be followed so as to formulate the problem in terms of the Euler – Lagrange equation are the following: i) Choose an origin of coordinates; ii) Define the degrees of freedom; iii) Define position and speed vectors; iv) Estimate the kinetic energy; v) Estimate the potential energy (elastic plus gravitational); vi) Estimate the non-conservative forces; vii) Assemble the equation

2.2.1 Origin of coordinates

The problem of one base fixed tank and another base isolated tank may be idealized by the following schemes, by putting two punctual masses (impulsive and convective) pursuant to the Housner model. The FPS isolators may be characterized by the curvature radium of a concave surface, which defines the isolation period, and by the friction coefficient in the sliding surface, which defines the energy dissipation and the system dampening; while it is variable in time with the sliding speed and the contact pressure, for this case, it is supposed to be constant. The isolator is modeled by a rigid bar with the same radius than the concave sliding surface. Said bar is articulated in both ends and connected to another horizontal rigid bar which represents the tank base, where a rigid vertical bar is then built, representing the walls of the anchored tank, and which is connected to the two Housner masses representing the contained liquid. The origin of coordinates is placed in the union of the rigid vertical bar (wall) and the rigid horizontal bar (bottom).

2.2.2 Degrees of freedom

The problem of the isolated tank shows two degrees of freedom, which correspond to the horizontal displacements of the two masses: the impulsive one (part of lower and medium water moving along with the rigid walls of the tank) with x_i displacement generated by the pendulum movement of the isolation system when being excited by a seism, and the convective one (part of upper water oscillating and generating waves in the free surface) with a x_c displacement. In the case of the base fixed tank, there is only one degree of freedom or independent displacement, which corresponds to the convective mass, since the impulsive mass is rigidly fixed to the tank walls and these are, in turn, anchored to the base, it has a displacement that coincides with the one from the ground during an earthquake. This is clearly observed when drawing the schemes in a deformed position in the Fig. 1.

As from here, the development will be followed only in the case of the isolated tank with two degrees of freedom. The case of the base fixed tank with only one degree of freedom may be obtained easily as from the first one or the model of base isolated can even be forced so as to work as a fixed base, by placing a curvature radius that is $R_c \approx 0$ and a friction coefficient that is μ=PGA.

The degrees of freedom, in terms of displacement, speed and acceleration, are:

$$\boldsymbol{q} = \begin{bmatrix} x_i \\ x_c \end{bmatrix} \quad (26) \qquad \boldsymbol{q_v} = \begin{bmatrix} v_i \\ v_c \end{bmatrix} = \begin{bmatrix} \dot{x}_i \\ \dot{x}_c \end{bmatrix} \quad (27) \qquad \boldsymbol{q_a} = \begin{bmatrix} a_i \\ a_c \end{bmatrix} = \begin{bmatrix} \ddot{x}_i \\ \ddot{x}_c \end{bmatrix} \quad (28)$$

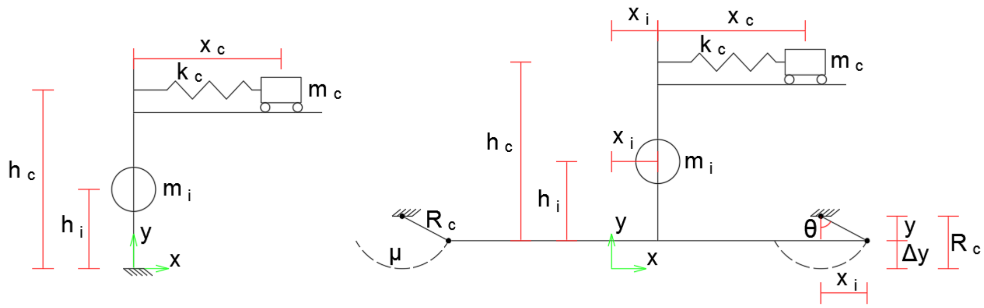

Fig. 1 – Degrees of freedom: base fixed (left) and base isolated (right)

The θ rotation and the Δy vertical displacement which generate the FPS isolators due to their pendulum movement, may be defined according to the x_i displacement of the impulsive mass.

As from the equation of a circle, "y" is found:

$$x_i^2 + y^2 = R_c^2 \qquad (29) \qquad\qquad y = \sqrt{R_c^2 - x_i^2} \qquad (30)$$

As from Fig. 1, Δy and θ are obtained:

$$\Delta y = R_c - y = R_c - \sqrt{R_c^2 - x_i^2} \quad (31) \qquad sen\theta = \frac{x_i}{R_c} \quad (32) \qquad \theta = arcsen\left(\frac{x_i}{R_c}\right) \quad (33)$$

2.2.3 Vectors of position and speed

The position of the impulsive and convective masses is defined regarding the chosen origin of coordinates, and according to the assigned degrees of freedom, giving the name of r_i to the impulsive position vector and r_c to the convective position vector. The "y" coordinate is obtained as the corresponding h height plus the Δy vertical displacement which are caused by the isolators.

$$\boldsymbol{r_i} = \begin{bmatrix} x_i \\ h_i + R_c - \sqrt{R_c^2 - x_i^2} \end{bmatrix} \quad (34) \qquad \boldsymbol{r_c} = \begin{bmatrix} x_i + x_c \\ h_c + R_c - \sqrt{R_c^2 - x_i^2} \end{bmatrix} \quad (35)$$

The speed vectors are obtained as from the previous ones by means of the use of Jacobian J to obtain the derivatives of the position vectors regarding the degrees of freedom.

$$\dot{\boldsymbol{r}} = \frac{\partial \boldsymbol{r}^T}{\partial \boldsymbol{q}} \dot{\boldsymbol{q}} = \boldsymbol{J}\dot{\boldsymbol{q}} \qquad (36)$$

2.2.4 Kinetic energy

The kinetic energy is calculated for each mass of the system, along with its corresponding speed vector.

$$T(\boldsymbol{q}, \dot{\boldsymbol{q}}) = \sum_{k=1}^{L} \frac{1}{2} \dot{\boldsymbol{r}}_k^T m_k \dot{\boldsymbol{r}}_k = \sum_{k=1}^{L} \frac{1}{2} (J_k \dot{\boldsymbol{q}})^T m_k (J_k \dot{\boldsymbol{q}}) \qquad (37)$$

2.2.5 Potential energy

The V_g gravitational potential energy (present in the two masses when arising due to the isolators) and the V_s elastic potential energy (present in the spring of the convective mass). Then, the two contributions are added.

$$V_g(\boldsymbol{q}) = \sum_{k=1}^{L} m_k g r_{2,k} \quad (38) \qquad\qquad V_s(\boldsymbol{q}) = \sum_{k=1}^{L} \frac{1}{2} u_k^T m_k u_k \quad (39)$$

2.2.6 Non-conservative forces

In this problem, there are two conservative forces dissipating energy, F_a force of dampening in the water connective movement and F_r force corresponding to the friction in the friction pendulum isolators:

$$F_a = -c_c v_c sign(v_c) \qquad (40) \qquad c_c = 2m_c\omega_c\xi_c \qquad (41)$$

$$F_r = -\mu N sign(v_i) \qquad (42) \qquad N = mgcos\theta + \frac{m{v_t}^2}{R} = m\left[gcos\theta + \frac{(v_i cos\theta)^2}{R}\right] \qquad (43)$$

These forces must be projected regarding the degrees of freedom, and for them, the work they perform is calculated (position vector of the application point multiplied by the force vector) and then it is derived regarding the degrees of freedom.

The friction force of the pendulum deserves a more detailed analysis. The normal intervening force varies inversely with the θ rotation angle and it is the addition of the weight radial component and the centripetal force. The sense of the friction force is contrary to the sense of speed force.

2.2.7 Euler Lagrange equation

The Euler-Lagrange equation may be interpreted as the addition of different terms of forces in equilibrium, since the system energies are derived regarding the degrees of freedom:

$$\frac{d}{dt}\left(\frac{\partial T}{\partial \dot{q}_j}\right) - \frac{\partial T}{\partial q_j} + \frac{\partial V}{\partial q_j} = {Q_j}^{NC} \quad \rightarrow \quad A - B + C = D \qquad (44)$$

$$\frac{d}{dt}\left(\frac{\partial T}{\partial \dot{q}_j}\right) = \frac{\partial}{\partial \dot{q}_j}\left(\frac{\partial T}{\partial \dot{q}_j}\right)\ddot{q}_j + \frac{\partial}{\partial q_j}\left(\frac{\partial T}{\partial \dot{q}_j}\right)\dot{q}_j \quad \rightarrow \quad A = A1 + A2 \qquad (45)$$

By adding the F_S external seismic force to the addition of the EL total force, the result is showed in Eq. (46). Since the system must be in dynamic equilibrium, the addition of all the internal and external forces must be null, the result is showed in Eq. (47):

$$EL = A1 + A2 - B + C - D + Fs \qquad (46) \qquad EL = A1 + A2 - B + C - D + Fs = 0 \qquad (47)$$

In this way, two differential equations of second order are obtained, since the problem shows two degrees of freedom.

2.3 State equation

As from the two Euler-Lagrange equations obtained, the acceleration of the impulsive and convective masses is intended to be solved. For this, an L linear matrix is assembled by putting the terms accompanying the accelerations that are looked for. This matrix is the mass matrix assessed in q=0. Then, the non-linear part of the equations may be expressed as:

$$NL = EL - a.L \qquad (48)$$

Remembering that EL=0, the acceleration must be solved as:

$$a = -L^{-1}.NL \qquad (49) \qquad \begin{bmatrix}\ddot{x}_i \\ \ddot{x}_c\end{bmatrix} = \begin{bmatrix} f_1(x_i, x_c, \dot{x}_i, \dot{x}_c) \\ f_2(x_i, x_c, \dot{x}_i, \dot{x}_c)\end{bmatrix} \qquad (50)$$

By making a change to state variables and their derivatives, the problem must be taken to a state equation with the form:

$$\dot{\boldsymbol{X}}(t) = \boldsymbol{A}.\boldsymbol{X}(t) + \boldsymbol{B}.\boldsymbol{f}(t) \qquad (51)$$

Where X is the state vector, f is the input vector (ground acceleration), A is the state matrix and B is the input matrix. In this way, instead of solving two ordinary differential equations of second order, four ordinary differential equations of first order are solved:

$$\begin{bmatrix}\dot{x}_i \\ \dot{x}_c \\ \ddot{x}_i \\ \ddot{x}_c\end{bmatrix} = \frac{d}{dt}\begin{bmatrix}x_i \\ x_c \\ \dot{x}_i \\ \dot{x}_c\end{bmatrix} = \begin{bmatrix}\dot{x}_i \\ \dot{x}_c \\ f_1(x_i, x_c, \dot{x}_i, \dot{x}_c) \\ f_2(x_i, x_c, \dot{x}_i, \dot{x}_c)\end{bmatrix} \qquad (52)$$

The problem must be solved now by integrating the four differential equations and defining four initial conditions of the variables that are looked for. In this way, the two displacements (both impulsive and convective) of the system and their corresponding speeds are obtained.

2.4 Numerical integration

The explicit Runge Kutta method of order 3 is used:

$$y_{n+1} = y_n + \frac{h}{4}(K_1 + 2K_2 + K_3) \quad (53) \qquad K_1 = f(t_n, y_n) = f_n \quad (54)$$

$$K_2 = f(t_n + \frac{h}{2}, y_n + K_1\frac{h}{2}) \quad (55) \qquad K_3 = f(t_n + h, y_n - K_1 h + 2K_2 h) \quad (56)$$

This method enables to numerically integrate the differential equations. The following value (y_{n+1}) is stated by this value (y_n) plus the product of the interval size (h) multiplied by an estimated slope. The slope is a weighted average of slopes, where K_1 is the slope at the beginning of the interval; K_2 is the slope in the medium point of the interval, by using K_1 so as to determine the "y" value in t_n+h/2 point by means of the Euler method; and K_3 is the slope at the end of the interval, with "y" value determined by K_2. The three slopes are averaged by assigning a higher weight to the slope at a medium point.

2.5 System of FPS isolation

The frictional pendulum isolators are the most advisable to be placed in the base of liquid storage tanks, since the T_b isolation period only depends on the R_c curvature radius of the sliding concave surface, and therefore, it keeps being constant, although the tank weight changes due to variations in the level of the contained liquid.

The force developed in the isolator is the sum of the restoring force, generated by the tangential component of the W weight, acting over the curved surface, and a friction force, caused by the reaction of the normal component of weight, acting over the curved surface. The restoring force controls the system rigidity according to the R_c curvature radius of the sliding concave surface, and the friction force controls the dampening of the system according to the µ friction coefficient between the slider and the sliding concave surface. The isolation period and the force developed in the isolator are obtained as:

$$T_b = 2\pi\sqrt{\frac{R_c}{g}} \quad (57) \qquad F_b = \frac{W}{R_c}\,x + \mu\, W\, sign\, \dot{x} \quad (58)$$

During the isolator operation, the W axial load may vary by the addition to the weight of the effects of seismic increase, which generates the structure overturning momentum, and by the vertical component of the ground acceleration. On the other hand, the µ friction coefficient may vary pursuant to the sliding speed and to the normal pressure over the sliding surface. In this article, for simplicity, said variations are not considered and are assumed as constant values. These effects must be included in a more complete analysis, for future research.

The friction coefficient increases quickly with the sliding speed until a certain value, beyond which it stays almost constant. In the case of contact between a Teflon slider and a stainless steel sliding surface, this effect is explained as follows. At low speeds and after the initial cycle, a very thin layer of Teflon is transferred to the stainless steel and the sliding occurs between both pieces of Teflon. At high speeds, big Teflon flakes are taken off the surface and grinded in the sliding interphase without being transferred to the steel, which derives in more friction. The increase of the friction coefficient with speed tends to stabilize at speeds around 10 cm/s.

On the other hand, the friction coefficient is reduced with the contact pressure increase on the slider, up to a limit value beyond which it stays constant. The effect of the friction coefficient with pressure is less intuitive. As the pressure between the material sheets increase, the contact area increase is lower than the normal load increase, and therefore, the friction force increase is lower than the vertical load increase, and as the friction coefficient is the quotient between friction force and vertical load, its value decreases.

2.6 Parametric analysis

In steps 2.1 to 2.4, the method used to solve the problem is explained. Said steps have been programmed in the MATLAB software so as to enable a fast method application when the data of a problem is modified. In this article, a parametric analysis is performed, using the maximum values obtained from the analysis of the response history, so as to determine the influence of the isolation period, the friction coefficient of the FPS isolators and the slenderness ratio (H/R) of the tank in the seismic response of the latter when it has its base isolated. The effectiveness of the isolation system is also analyzed by comparing the base fixed tank response. Different values are adopted for the abovementioned parameters. For the isolation period, 3.0s, 3.5s, 4.0s and 4.5s are taken. For the friction coefficient, 0.05, 0.10, 0.15 and 0.20 are taken. For the slenderness ratio, 0.5, 1.0, 1.5 and 2.0 are taken. Four seismic registries are used as an input for the system, so as to perform an analysis of the response history. Three of them has subduction origin (Algarrobo, Maule, Tōhoku) and one of them corresponds to a transcurrent near fault with impulsive characteristics (Landers).

Table 1 – Seismic registries used in the analysis

Earthquake place	Date	Momentum magnitude (Mw)	Registry station	Registry component	PGA registry [g]	Registry duration [s]	Registry time step [s]
Algarrobo, Chile	03-03-1985	8.0	Llolleo	E-W	0.71	116.38	0.005
Landers, United States	28-06-1992	7.3	SCE24	N-S	0.78	48.09	0.01
Maule, Chile	27-02-2010	8.8	Constitución	E-W	0.54	143.27	0.005
Tōhoku, Japan	11-03-2011	9.0	FKS016	N-S	1.22	299.99	0.01

The response is quantified by taking as an output the relative displacement of the convective mass (x_c), the relative displacement of the isolation system (x_b) that, due to the considerations performed in the model (rigid connection of the tank base to the also rigid walls) is equal to the displacement of the impulsive mass (x_i), and the normalized base shear (that may be interpreted as the seismic coefficient or the effective acceleration of the system in the base that is expressed as a fraction of gravity acceleration). This last parameter is obtained in the case of the isolated base from Eq. (58) and for the fixed base case from the Housner proposed equation:

$$F_b = \sqrt{(S_{ai}.m_i)^2 + (S_{ac}.m_c)^2} \tag{59}$$

Where S_{ai} and S_{ac} are the spectral ordinates corresponding to the period of impulsive and convective masses, respectively. As the impulsive mass is rigidly connected to the floor (tank walls with no flexibility), S_{ai} = PGA. Equation for F_b is conservative, since the maximum response of each vibration mode (impulsive and convective) is not produced at the same moment.

3. Results

3.1 Incidence of the isolation period in the tank response

Broad tank (H/R=0.50) Slender tank (H/R=2.00)

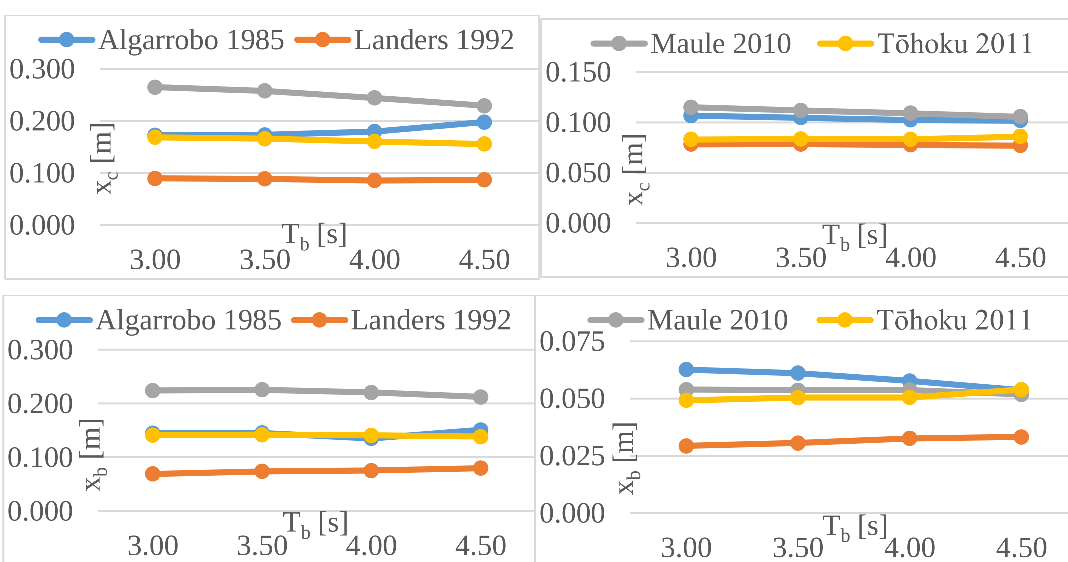

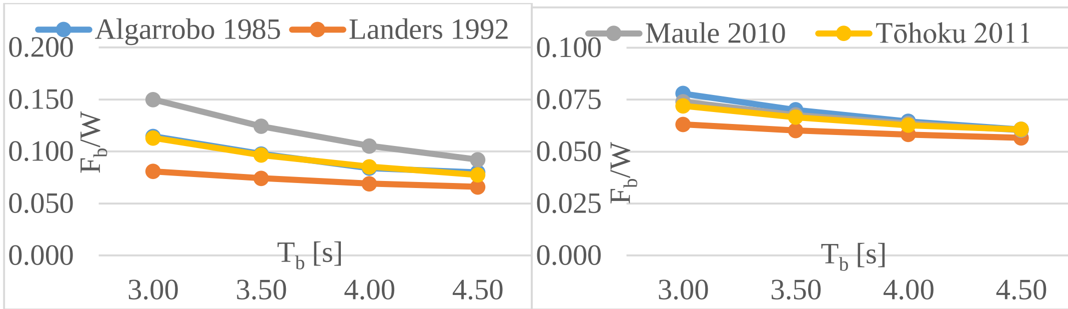

Fig. 2 – Variation of the x_c convective displacement, the x_b isolator displacement and the F_b/W normalized base shear with the change of T_b isolation period, for a broad tank (left) and for another slender tank (right) with a μ friction coefficient that is constant and equal to 0.05

It is observed that, in most seismic registries used, the increase in the isolation period does not generate a noticeable reduction in the displacement of the tank convective mass, in charge of the swell in the free surface. It is clearly exposed that the increase of the isolation period leads to a significant reduction of the normalized base shear. Finally, it is noticed that, in all cases, the responses are lower for the slender tank than for the broad one.

3.2 Incidence of the friction coefficient in the tank response

Broad tank (H/R=0.50) Slender tank (H/R=2.00)

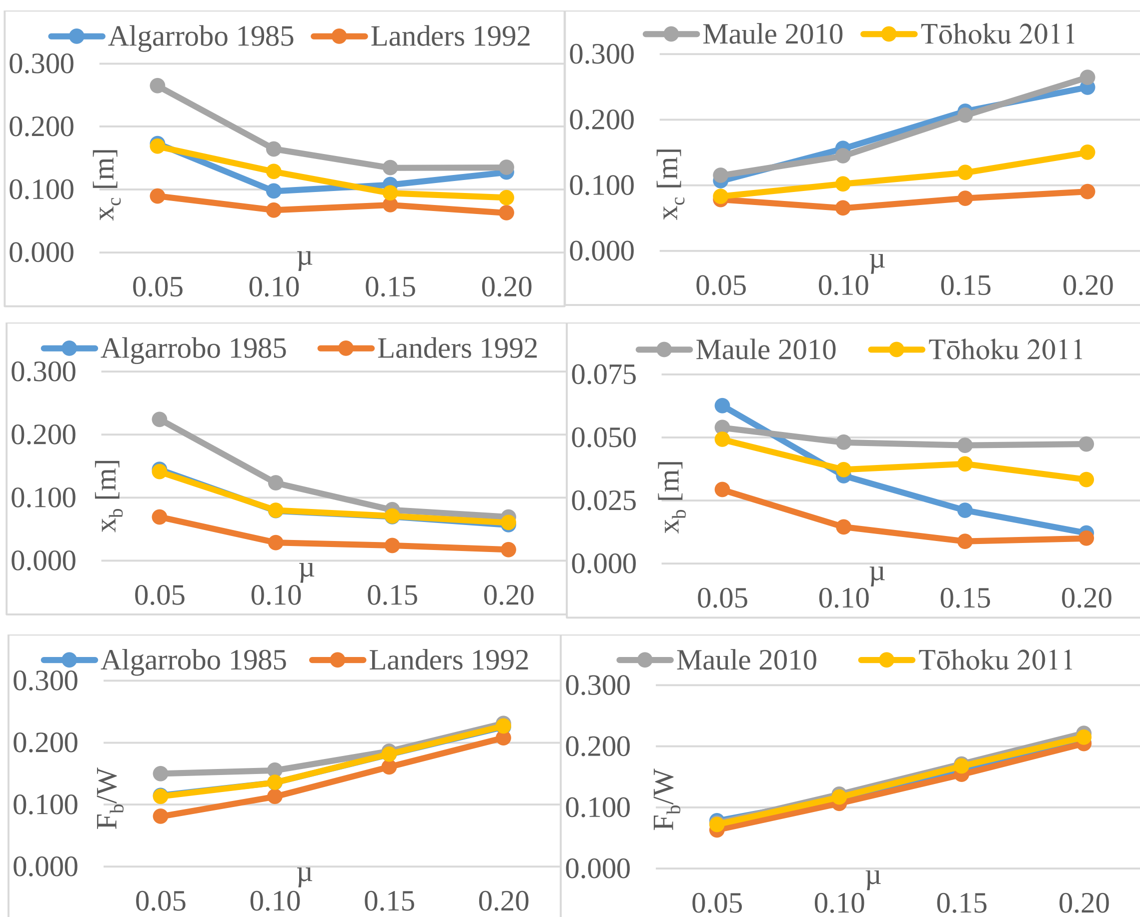

Fig. 3 – Variation of the x_c convective displacement, the x_b isolator displacement and the F_b/W normalized base shear with the change of the μ friction coefficient, for a broad tank (left) and for another slender tank (right) with an T_b isolation period that is constant and equal to 3.00s

It is observed that the increase of the friction coefficient has different effects according to the tank slenderness, causing a decrease of the convective displacement for broad tanks and its increase for the slender tanks. On the other hand, a higher friction coefficient decreases the isolator displacement and considerably increases the normalized base shear.

3.3 Incidence of the slenderness ratio in the tank response

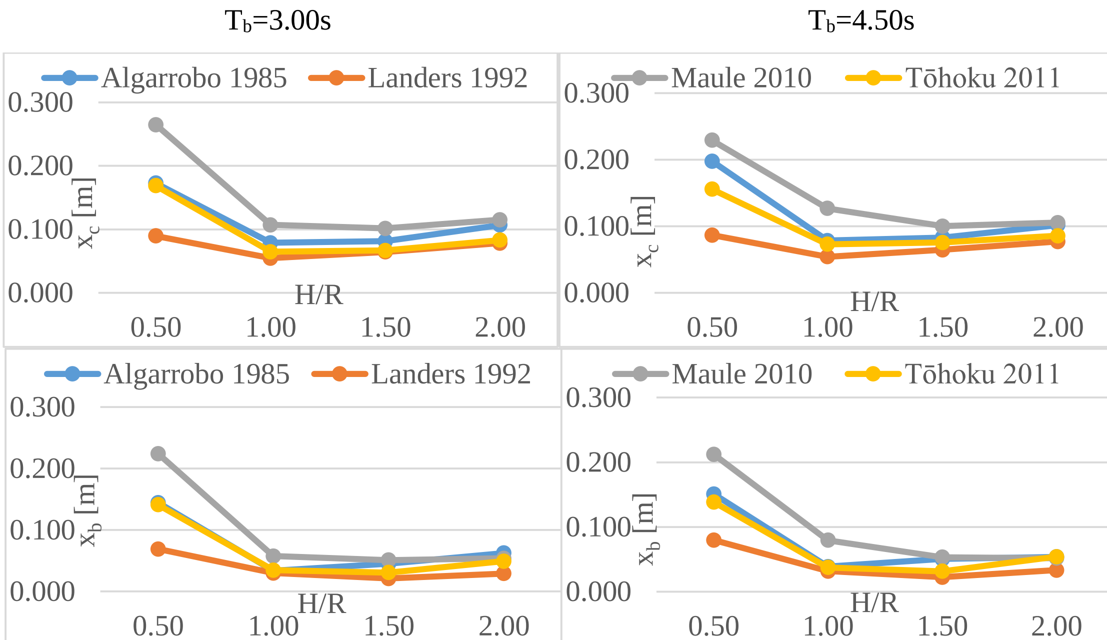

Fig. 4 – Variation of the x_c convective displacement and the x_b isolator displacement, for an isolation period that is T_b=3.00s (left) and another T_b=4.50s period (right) with a μ friction coefficient that is constant and equal to 0.05s

It is observed that the slender tanks show low responses.

3.4 Effectiveness of the isolation system

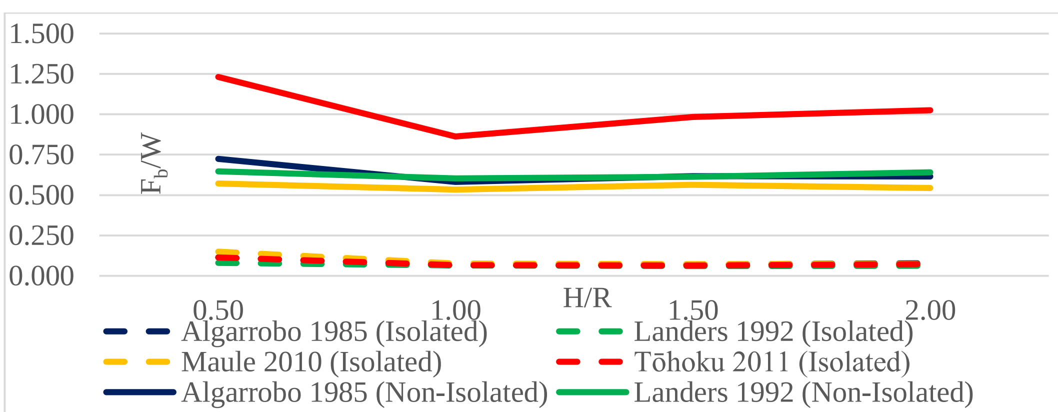

Fig. 5 – Variation of the F_b/W normalized base shear with the change of the slenderness ratio for a non-isolated tank and for an isolated tank with an isolation period that is T_b=3.00s and a friction coefficient that is μ=0.05

The isolation system has proved to be effective with all the registries, increasing the reduction of the base shear with the increase of the slenderness ratio.

4. Conclusions

As from the result analysis, it is concluded that: a) the technique of seismic isolation is effective to reduce the tank response; b) the response reduction increases with the slenderness ratio, and this is because, in slender tanks, the impulsive component of low period is the one controlling the response, and therefore, it is affected when the system period increases. In broad tanks, on the other hand, the convective component is of most importance, and since it has a superior period compared to the isolation system, no big reductions in the response are appreciated; c) the increase of the isolation period significantly reduces the response in terms of accelerations, but its incidence over the convective displacement, in charge of the swell in the free surface, is not determinant; d) the increase of the friction coefficient reduces the effectiveness of the isolation system in terms of accelerations, by increasing the normalized base shear, but it causes a reduction of the convective displacement in broad tanks, due to its dampening effect over the system; e) the friction coefficient turns to be a key parameter to balance the response of broad tanks, between a reduction of baseline acceleration and an increase of convective displacement. The optimum value of said coefficient must be analyzed for each particular seismic registry.

5. References

[1] Westergaard HM (1933): Water pressures on dams during earthquakes. *Transactions of the American Society of Civil Engineers*, 98 (2), 418-433.

[2] Jacobsen LS (1949): Impulsive hydrodynamics of fluid inside a cylindrical tank and of fluid surrounding a cylindrical pier. *Bulletin of the Seismological Society of America*, 39 (3), 189-204.

[3] Housner GW (1957): Dynamic pressures on accelerated fluid containers. *Bulletin of the Seismological Society of America*, 47 (1), 15-35.

[4] Housner GW (1963): The dynamic behavior of water tanks. *Bulletin of the Seismological Society of America*, 53 (2), 381-387.

[5] Veletsos AS (1973): Seismic effects in flexible liquid storage tanks. *Proceedings of Fifth World Conference on Earthquake Engineering*, 1, 630-639.

[6] Haroun MA, Housner GW (1981): Earthquake response of deformable liquid storage tanks. *Journal of Applied Mechanics*, 48 (2), 411-418.

[7] Haroun MA (1983): Vibration studies and tests of liquid storage tanks. *Earthquake Engineering and Structural Dynamics*, 11 (2), 179-206.

[8] Malhotra PK (1997): New method for seismic isolation of liquid-storage tanks. *Earthquake Engineering & Structural Dynamics*, 26 (8), 839-847.

[9] Wang YP, Teng MC, Chung KW (2001): Seismic isolation of rigid cylindrical tanks using friction pendulum bearings. *Earthquake Engineering & Structural Dynamics*, 30 (7), 1083-1099.

[10] Shrimali MK, Jangid RS (2002): Non-linear seismic response of base-isolated liquid storage tanks to bi-directional excitation. *Nuclear Engineering and Design*, 217 (1), 1-20.

[11] Panchal VR, Jangid RS (2008): Variable friction pendulum system for seismic isolation of liquid storage tanks. *Nuclear Engineering and Design*, 238 (6), 1304-1315.

[12] Panchal VR, Jangid RS (2012): Behaviour of liquid storage tanks with VCFPS under near-fault ground motions. *Structure and Infrastructure Engineering*, 8 (1), 71-88.

[13] Abalı E, Uçkan E (2010): Parametric analysis of liquid storage tanks base isolated by curved surface sliding bearings. *Soil Dynamics and Earthquake Engineering*, 30 (1), 21-31.

[14] Saha SK, Matsagar VA, Jain AK (2014): Earthquake response of base-isolated liquid storage tanks for different isolator models. *Journal of Earthquake and Tsunami*, 8 (5), 1-22.

[15] Almazán JL (2014): Demostración de las ecuaciones de Euler-Lagrange a partir del Principio de Trabajos Virtuales y la Segunda Ley de Newton. *Apuntes Dinámica Computacional ICE 3733*. Pontifica Universidad Católica de Chile.